Appl Microbiol Biotechnol (2015) 99:6481–6491
DOI 10.1007/s00253-015-6524-2

ENVIRONMENTAL BIOTECHNOLOGY

Ammonia manipulates the ammonia-oxidizing archaea and bacteria in the coastal sediment-water microcosms

Yan Zhang[1,4] · **Lujun Chen**[1,3] · **Tianjiao Dai**[2] · **Renhua Sun**[2,5] · **Donghui Wen**[2]

Received: 3 February 2015 / Revised: 2 March 2015 / Accepted: 3 March 2015 / Published online: 24 March 2015

Abstract Ammonia was observed as a potential significant factor to manipulate the abundance and activity of ammonia-oxidizing microorganisms (AOMs) in water environments. For the first time, this study confirmed this phenomenon by laboratory cultivation. In a series of estuarine sediment-coastal water microcosms, we investigated the AOM's phylogenetic composition and activity change in response to ammonia concentration. Increase of ammonia concentration promoted bacterial *amoA* gene abundance in a linear pattern. The ratio of transcribed ammonia-oxidizing bacteria (AOB) *amoA* gene/ammonia-oxidizing archaea (AOA) *amoA* gene increased from 0.1 to 43 as NH_4^+-N increased from less than 0.1 to 12 mg L^{-1}, and AOA *amoA* transcription was undetected under 20 mg NH_4^+-N L^{-1}. The incubation of stable isotope probing (SIP) microcosms revealed a faster ^{13}C-$NaHCO_3$ incorporation rate of AOA *amoA* gene under 0.1 mg NH_4^+-N L^{-1} and a sole ^{13}C-$NaHCO_3$ utilization of the AOB *amoA* gene under 20 mg NH_4^+-N L^{-1}. Our results indicate that ammonia concentration manipulates the structure of AOM. AOA prefers to live and perform higher *amoA* transcription activity than AOB in ammonia-limited water environments, and AOB tends to take the first contributor place in ammonia-rich ones.

Keywords Ammonia-oxidizing archaea · Ammonia-oxidizing bacteria · Sediment microcosm · Stable isotope probing · Transcriptional activity

Introduction

Nitrification is the only oxidative process that links the reduced and oxidized pools of inorganic nitrogen to sustain the global nitrogen cycle (Leininger et al. 2006). Aerobic ammonia oxidation, the first and rate-limiting step in nitrification, thus plays an integral role for the global nitrogen balance. Ammonia-oxidizing bacteria (AOB) as well as recently discovered ammonia-oxidizing archaea (AOA) (Francis et al. 2005; Konneke et al. 2005; Venter et al. 2004) are two distinct ammonia-oxidizing microorganisms (AOMs) that catalyze the oxidation of ammonia to hydroxylamine and further to nitrite. Both AOMs demonstrate wide distribution in terrestrial (Adair and Schwartz 2008; Le Roux et al. 2008; Wessen et al. 2011), freshwater (Liu et al. 2013; Wu et al. 2010), and marine environments (Beman et al. 2010; Bouskill et al. 2012; Mosier and Francis 2008).

Oceans cover 71 % of the earth's surface and contain enormous biomass and large biodiversity; thus, marine microorganisms are a crucial component in global nutrient cycles (Arrigo 2005). Influenced by many environmental factors, such as salinity (Caffrey et al. 2007), dissolved oxygen (DO) (Bouskill et al. 2012; Molina et al. 2010), and ammonia

Electronic supplementary material The online version of this article (doi:10.1007/s00253-015-6524-2) contains supplementary material, which is available to authorized users.

✉ Donghui Wen
dhwen@pku.edu.cn

[1] School of Environment, Tsinghua University, Beijing 100084, China

[2] College of Environmental Sciences and Engineering, Peking University, Beijing 100871, China

[3] Zhejiang Provincial Key Laboratory of Water Science and Technology, Department of Environmental Technology and Ecology, Yangtze Delta Region Institute of Tsinghua University, Jiaxing, Zhejiang 314050, China

[4] Department of Civil & Environmental Engineering, University of Alberta, Edmonton, Alberta T6G 2W2, Canada

[5] Rural Energy & Environment Agency, Ministry of Agriculture, Beijing 100125, China

concentration (Wuchter et al. 2006), the abundance and activity of AOA and AOB varied in different marine environments. Among these factors, ammonia has been identified as one of the most significant factors structuring AOM ecosystems. A time series study in the North Sea revealed that the abundance of AOA *amoA* gene was negatively correlated with ammonium concentration (3–12.7 μM) (Wuchter et al. 2006). Physiological study of the first isolated AOA strain demonstrated that the ammonia substrate threshold for AOA was considerably lower than that for AOB (Martens-Habbena et al. 2009). Therefore, an acceptable hypothesis could be proposed that AOA may contribute more to nitrification in environments with low ammonia concentration but AOB may be more favorable in environments with high ammonia concentration.

The same phenomenon of AOA and AOB influenced by ammonia concentration was found in soil environment (Glaser et al. 2010). More importantly, pieces of evidence for the above hypothesis have been provided by Di et al. (Di et al. 2010; Di et al. 2009), Verhamme et al. (Verhamme et al. 2011), and Pratscher et al. (Pratscher et al. 2011) in lab simulating microcosms for soil environment. Unfortunately, in aquatic environments, the hypothesis has not been confirmed yet in laboratory cultivation system, and the dynamics of phylogenetic diversity of active AOA and AOB under different ammonia concentrations is still unclear. Hence, the influence of ammonia concentration on the activities of aquatic AOA and AOB needs to be further verified, especially as terrestrial and marine species mainly belong to different lineages.

By setting up estuarine sediment-coastal water microcosms with a series of ammonia concentrations, this study aims to address the critical knowledge gaps in understanding the transcriptional activity of AOA and AOB and the dynamics of phylogenetic diversity of active AOA and AOB at different ammonia concentrations in aquatic environments. Molecular technologies of quantitative PCR (qPCR), quantitative reverse transcription PCR (RT-qPCR), and 454 pyrosequencing were applied to track precisely the archaeal and bacterial *amoA* genes. On the basis of chemolithotrophic ammonia oxidation carried out by AOA and AOB (Jia and Conrad 2009; Pratscher et al. 2011; Xia et al. 2011; Zhang et al. 2010), DNA-stable isotope probing (SIP) was also adopted to reveal potential active AOA and AOB who absorbed inorganic carbon in the coastal microcosms.

Materials and methods

Sediment sampling and characteristics measurement

The sediment and coastal water samples used for microcosms' incubation were collected from the Hangzhou Bay at the site of N 30° 12.780′, E 120° 51.144′, using a sediment sampler (Van Veen, HYDRO-BIOS, Germany). The sediment properties were as follows: water content 31.6 %, pH 8.53, total organic carbon (TOC) 361.4 mg g^{-1} dried sediment, ammonia nitrogen (NH_4^+-N) 22.69 μg g^{-1} dried sediment, nitrite nitrogen (NO_2^--N) no detection, nitrate nitrogen (NO_3^--N) 2.89 μg g^{-1} dried sediment, and total phosphorus (TP) 0.53 mg g^{-1} dried sediment. The water quality was as follows: pH 7.80, DO 5.82 mg L^{-1}, salinity 5.36 psu, chemical oxygen demand (COD) 3.07 mg L^{-1}, NH_4^+-N 0.17 mg L^{-1}, NO_2^--N 0.03 mg L^{-1}, NO_3^--N 2.89 mg L^{-1}. The methods adopted for the detection of samples' characteristics were listed in Table S1.

Microcosm incubation

The laboratory microcosms were constructed in a series of 120 mL Erlenmeyer flasks, each with 10 g sediment and 50 mL coastal water sample sealed with sterile sealing film. The microcosms were incubated under five different coastal water NH_4^+-N concentrations of 0.1, 2, 6, 12, and 20 mg L^{-1}, maintained by supplementing ammonium sulfate to the designed concentration after determining the demands every morning. For example, as the ammonium in microcosms with NH_4^+-N concentrations of 0.1 mg L^{-1} could be consumed completely in 24 h, 0.1 mg NH_4^+-N L^{-1} was supplemented into the microcosms everyday. The microcosm without additional ammonium sulfate was constructed as the control. The total amounts of NH_4^+-N supplemented into the microcosms are listed in Table S2. Triplicate microcosms were constructed for each NH_4^+-N concentration. Six groups of the microcosms with NH_4^+-N concentration from 0 (the control) to 20 mg L^{-1} were coded as A0, A0.1, A2, A6, A12, and A20. Microcosms were incubated at 25 °C in dark and mixed by shaking every morning for air exchange to maintain aerobic condition. At the day 28, approximate 4 g of the cultivated sediment in each microcosm were sampled and frozen at −70 °C immediately for further analysis. After 56-day cultivation, all the cultivated sediments were collected, parts of each sample were used to RNA extraction immediately, and the remaining sediment was frozen at −70 °C for further analysis. The aqueous phases after 56-day cultivation were used for water quality analysis.

Stable isotope probing of potential active ammonia oxidizers

The DNA-SIP microcosms were constructed in 120-mL serum bottles with 10 g sediment and 50 mL coastal water sample sealed with rubber stoppers and plastic caps. Low (0.1 mg L^{-1}) and high (20 mg L^{-1}) NH_4^+-N concentrations were designed for DNA-SIP study. The NH_4^+-N concentrations were maintained by supplementing ammonium sulfate into the microcosms every morning. The total amounts of NH_4^+-N supplemented into the microcosms are also listed in

Table S2. The air in the headspace of each bottle was replaced with synthetic air (80 % N_2 and 20 % O_2) to remove CO_2 from the microcosms, and external bicarbonates were added to the microcosms as the additional inorganic carbon (IC) sources. At each NH_4^+-N concentration, two groups of microcosms were supplemented respectively by two IC sources, 100 mg L^{-1} $NaH^{12}CO_3$ and 100 mg L^{-1} $NaH^{13}CO_3$ (Sigma-Aldrich Co., St Louis, MO, USA). The initial pH of the microcosms was shown in Table S3. The sodium bicarbonates were complemented into the corresponding microcosms every 2 weeks. Four groups of the SIP microcosms were coded as ^{12}C-0.1, ^{12}C-20, ^{13}C-0.1, and ^{13}C-20. Duplicate microcosms of each group were incubated at 25 °C in the dark. Sediments after 28 and 56-day cultivation were sampled and frozen at −70 °C immediately for further analysis. The aqueous phases after 56-day cultivation were collected for water quality analysis.

Nucleic acid extraction and reverse transcription

DNA was extracted from 0.5 g of sediment samples using the DNA PowerSoil® Total DNA Isolation Kit (Mo Bio, Carlsbad, CA). The concentration of extracted DNA was measured by a NanoDrop 2000 UV-Vis spectrophotometer (Thermo Fisher, Wilmington, MA, USA). RNA was extracted from 3 g of samples using the RNA PowerSoil® Total RNA Isolation Kit (Mo Bio, Carlsbad, CA). The extracted RNA solution was treated by DNase to eliminate the residual DNA using a RTS™ DNase Kit (Mo Bio, Carlsbad, CA) immediately, followed by reverse transcription with a PrimeScript™ RT reagent Kit (Takara, Dalian, China). The extracted DNA and the obtained complementary DNA (cDNA) were stored at −70 °C for further analysis.

SIP DNA fractionation

The DNA samples from the duplicate microcosms were mixed prior to fractionation. Density gradient centrifugation of the mixed DNA in CsCl gradients was performed as described by Neufeld et al. (Neufeld et al. 2007). Briefly, approximate 2 μg extracted DNA was combined into a 7.163 M CsCl gradient buffer to achieve an initial buoyant density of 1.72 g mL^{-1}. The ultracentrifugation of the mixed solution was performed in 5 mL OptiSeal polyallomer tubes with a VTi 90 vertical rotor (Beckman Coulter, Palo Alto, CA, USA) at 177,000 g_{av} for 40 h at 20 °C. Fourteen equal volumes were fractionated from centrifuged gradient by slowly loading air into the top of the tubes with needles and an Ismatec@ peristaltic pump (IDEX, Wertheim, Germany). After fractionation, the density of each fraction was determined by weighing method using an electronic analytical balance (XS105DU, METTLER TOLEDO, Switzerland) and a micropipette (Eppendorf, Germany). Nucleic acids were precipitated from CsCl gradients by polyethylene glycol 6000 (Wako, Japan) and glycogen (Fermentas, Canada) overnight and re-dissolved in 30 μL sterile water after washing with 70 % ethanol.

qPCR

Quantitative PCR was performed on an iCycler IQ5 thermocycler (Bio-Rad, CA, USA) based on SYBR Green I method. The primers and thermal programs for quantitative amplification of bacterial and archaeal *amoA* genes were listed in Table S4. Each reaction was performed in 20 μL, which consisted of 10 μL of SYBRs Premix Ex TaqTM (Takara, Dalian, China), 1.0 μL of template DNA, and 0.4 μL of primers. The standard plasmids for quantitative analysis were selected from the positive clones of the target genes amplified from the sediment sample, as described previously (Bai et al. 2012b). Tenfold serial dilutions of the plasmids DNA were subjected to a quantitative PCR assay in triplicate to generate a standard curve and to check the amplification efficiency. The correlation coefficients of the standard curves (R^2) were all >0.99, and the amplification efficiencies ranged from 94.8 to 104.7 %.

Pyrosequencing and phylogenetic analysis of *amoA* genes

The archaeal and bacterial *amoA* genes in the cDNA samples from non-SIP microcosms and the DNA samples from the heavy fractions of SIP microcosms were analyzed by pyrosequencing. The pyrosequencing was performed on a Roche GS-FLX Titanium Sequencer (Roche Diagnostics Corporation, Branford, CT) using a described process (Bai et al. 2012a). Briefly, the amplifications were achieved on an ABI9700 thermocycler (ABI, Foster City, USA) with barcoded primers, using TransStart Fastpfu DNA polymerase (TransGen, Beijing, China). The primers and thermal programs were listed in Table S4. After purifying the PCR products, the amplicon libraries were generated by emulsion PCR and sequenced on the Roche GS-FLX Genome Sequencer using the 454/Roche B sequencing primer kit. The pyrosequencing flowgrams were converted to sequence and analyzed with standard pipeline adopting QIIME software (Caporaso et al. 2010). Initially, low quality and ambiguous reads, i.e., the reads with ambiguous base >0, sequence lengths <440 bp, or average sequence quality <25, were eliminated by filtering and denoising after barcodes were removed from the sequence reads. Subsequently, putative chimeras were identified and removed from the pre-treated sequences with Chimera-uchime. Applying Mothur software (Schloss et al. 2009), the remained sequences were clustered into different OTUs with 97 % of sequence identity threshold for bacterial *amoA* gene (Gao et al. 2013; Wang et al. 2012) and 95 % for archeal *amoA* gene (Beman et al. 2008; Mosier and Francis 2008). Then, the rarefaction and diversity statistics

were calculated. The representative sequences in main OTUs were selected to blast with the National Center for Biotechnology Information (NCBI) database and obtain the closest sequences published in the NCBI. The phylogenetic trees of the selected OTUs and the closest sequences were constructed using the neighbor-joining method with the MEGA 5.2 software (Kumar et al. 2008). All original 454 sequences were archived at the NCBI Sequence Read Archive (SRA) under accession SRP035514.

Results

Microcosms' incubation with different ammonia concentrations

After incubation for 56 days, a significant increase of nitrate in the aqueous phase (Fig. 1) indicated the stimulation of nitrification in all microcosms; however, nitrite accumulated in the three microcosms supplemented with the higher ammonia concentrations, especially in A20 where final concentration of NO_2^--N (163.16±13.29 mg L^{-1}) was higher than that of NO_3^--N (63.20±5.79 mg L^{-1}) (P=0.000). Together, the total amount of accumulated nitrite- and nitrate-nitrogen increased from 6.69±0.14 to 226.36±7.92 mg L^{-1} as the NH_4^+-N concentration improved from control (less than 0.1 mg L^{-1}) to 20 mg L^{-1}.

In the beginning of the microcosm incubation, AOA ($8.94\times10^6\pm1.65\times10^6$ copies g^{-1}) was nearly one order of magnitude higher than AOB ($1.12\times10^6\pm2.11\times10^5$ copies g^{-1}) (P=0.001) in the sediments, as shown in Fig. 2. After

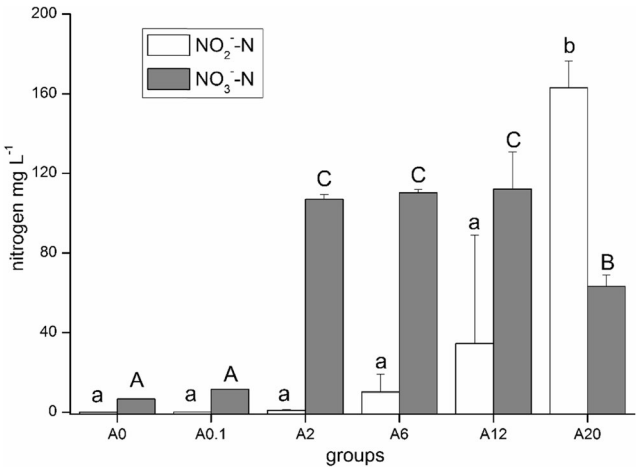

Fig. 1 Nitrite-N and nitrate-N in the aquatic phases of the microcosms after 56-day cultivation. Group "Ax" represents the microcosm with ammonia concentration of "x" mg L^{-1}. *Error bars* represent the standard deviations of the triplicate microcosms. *Different letters above the bars* (*lowercase letters* for nitrite-N, *capital letters* for nitrate-N) indicate a significant difference (P<0.05) by ANOVA analysis using Student-Newman-Keulstest method

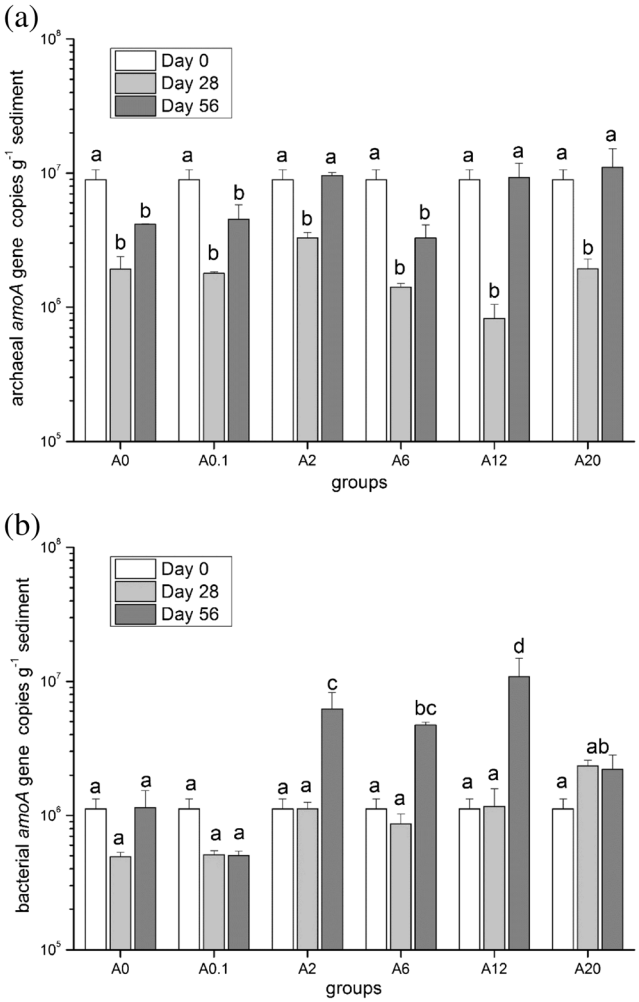

Fig. 2 Changes in the abundance of *amoA* genes in the sediments cultivated under different ammonia concentrations. *Error bars* represent standard errors of triplicate microcosms. *Different letters above the bars* indicate a significant difference (P<0.05). **a** Archaeal *amoA* and **b** bacterial *amoA*

28-day cultivation, the copy numbers of archaeal *amoA* gene dropped in all the sediments, fluctuating in a range from $8.23\times10^5\pm2.2\times10^5$ to $3.28\times10^6\pm3.18\times10^5$ copies g^{-1} sediment, while the copy numbers of bacterial *amoA* gene dropped only in the sediments of group A0 and A0.1 but maintained in group A2, A6, and A12 and even rose to $2.36\times10^6\pm2.35\times10^5$ copies g^{-1} sediment in group A20. After 56-day cultivation, the copy numbers of archaeal *amoA* gene recovered to $3.26\times10^6\pm8.44\times10^5$ to $4.49\times10^6\pm1.30\times10^6$ copies g^{-1} sediment in A0, A0.1 and A6, even exceeded the original quantity in A2, A12, and A20, while the copy numbers of bacterial *amoA* gene maintained in A0.1 and A20 and increased significantly in the other groups, even far exceeding the original quantity in group A2, A6, and A12.

Regression analysis (Fig. 3) showed that the archaeal *amoA* gene abundance had slightly negative correlation and moderate positive correlation with the NH_4^+-N concentration in day

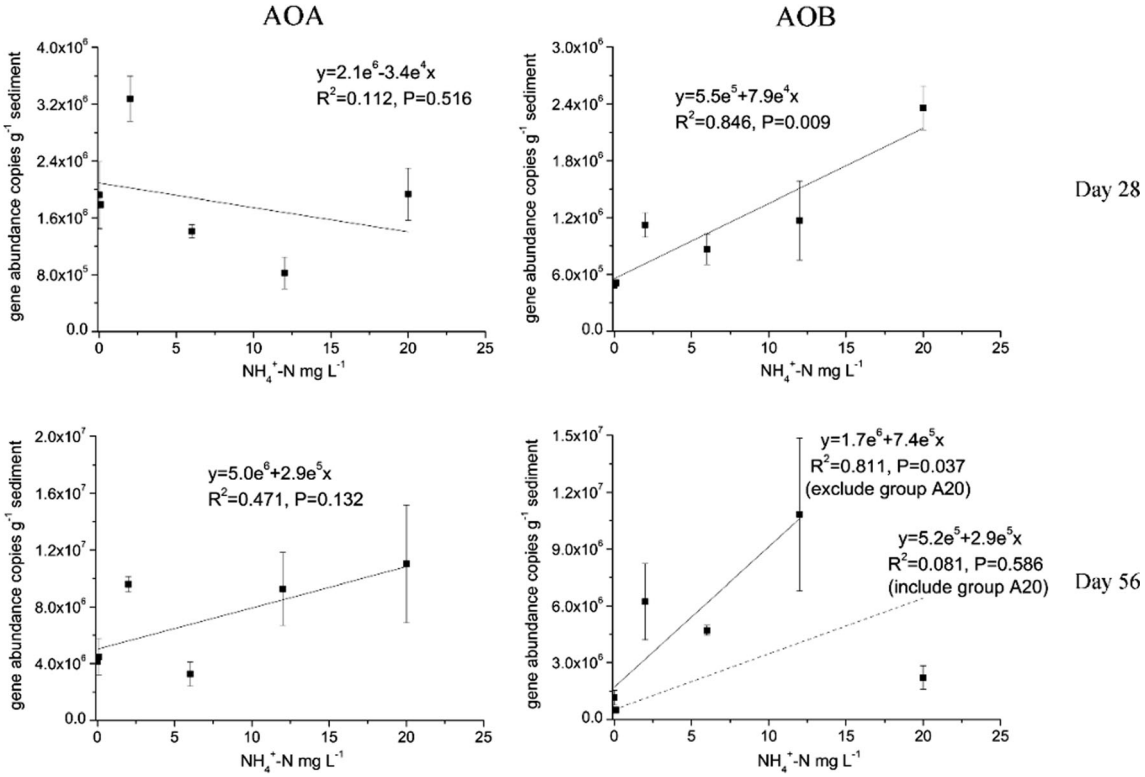

Fig. 3 Relationship between NH_4^+-N concentration and *amoA* gene copy numbers in the microcosms. *Vertical error bars* represent respectively the standard errors of *amoA* gene copies from triplicate microcosms

28 and day 56, respectively. However, significant positive correlations emerged between the bacterial *amoA* gene abundance and the NH_4^+-N concentration. In day 56, if excluding the data of group A20, such positive correlation became evident again.

The abundance of transcribed *amoA* genes measured by RT-qPCR was shown in Fig. 4. Archaeal *amoA* gene had more transcripts than bacterial at lower ammonia concentrations of group A0 (P=0.018) and A0.1 (P=0.074) but less transcripts than bacterial at the other higher ammonia concentrations. The abundance of transcribed bacterial *amoA* gene in group A0 (144±4 copies g^{-1} sediment) and A0.1 (281±103 copies g^{-1} sediment) were much lower than that in other groups ($8.9\times10^3\pm3.5\times10^3$ to $3.5\times10^5\pm3.9\times10^4$ copies g^{-1} sediment) (P= 0.049 and 0.051 for A0 and A0.1 comparing to A20, respectively). The transcribed archaeal *amoA* gene increased from group A0 to group A2 but decreased subsequently from group A2 to group A12 and finally was not detected in all three microcosms of group A20.

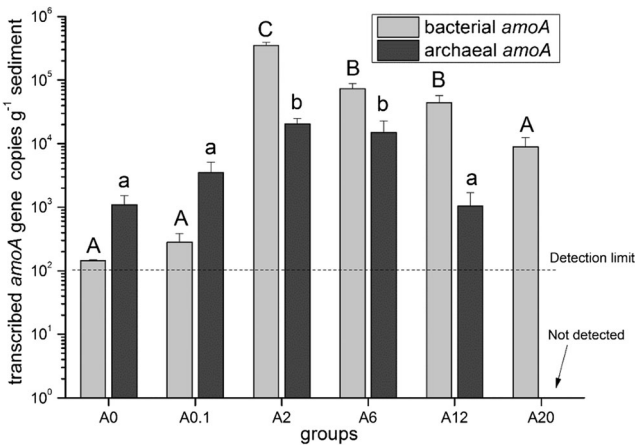

Fig. 4 Changes in the abundance of transcribed *amoA* genes in mRNA of the sediments cultivated under different ammonia concentrations after 56-day cultivation. *Error bars* represent the standard errors of triplicate microcosms. *Different letters above the bars* (*lowercase letters* for archaeal *amoA*, *capital letters* for bacterial *amoA*) indicate a significant difference (P<0.05)

DNA-SIP incubation

During the incubation of microcosms adding different C isotopes as the IC source, the changes of nitrite, nitrate concentrations, and the abundance of *amoA* genes in the ^{13}C-$NaHCO_3$ microcosm were consistent with that in the ^{12}C one, as Fig. 5 indicated.

Nitrification achieved in all SIP microcosms, especially under high ammonia concentration (Fig. 5a). Nitrate accumulated much more than nitrite under both low and high ammonia concentrations. The change of the abundance of archaeal *amoA* gene was different under the different ammonia concentrations (Fig. 5b). After 56-day cultivation, the archaeal *amoA* gene slightly increased in microcosms with 0.1 mg L^{-1} NH_4^+-

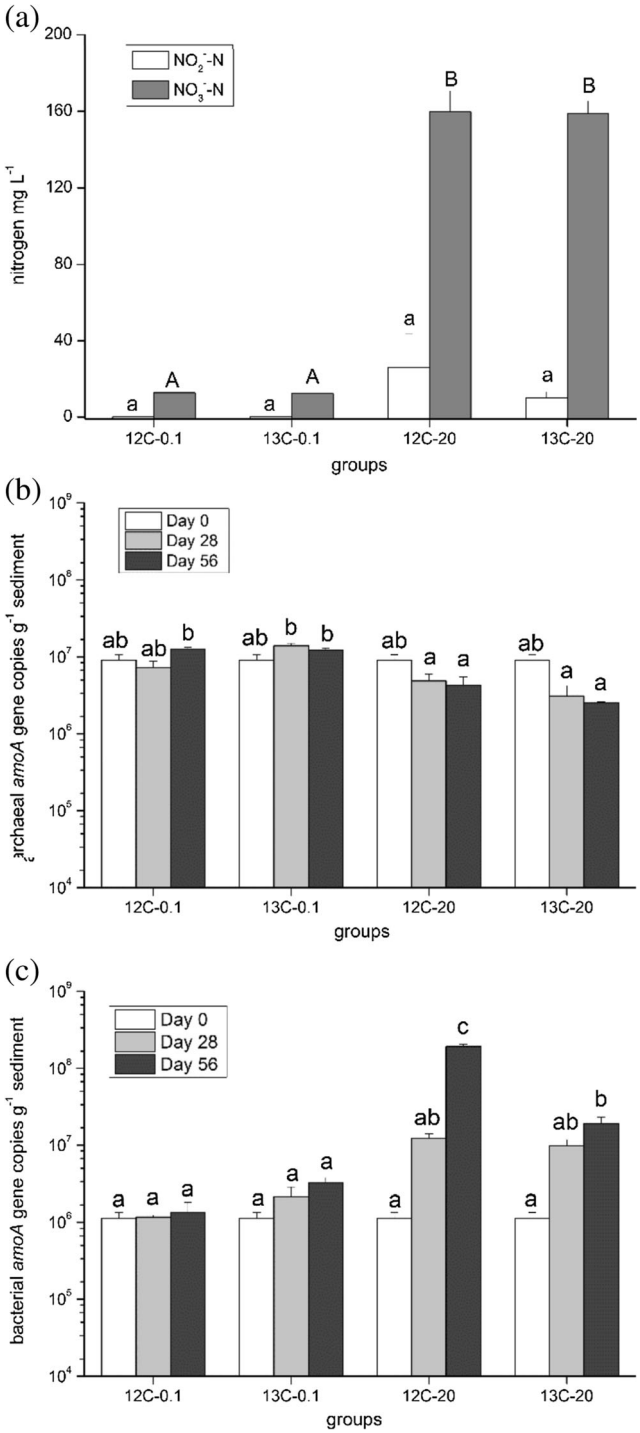

Fig. 5 DNA-SIP microcosms' incubation. **a** Nitrite-N and nitrate-N in SIP microcosms after 56-day cultivation; **b** change of the abundance of archaeal *amoA* gene; and **c** change of the abundance of bacterial *amoA* gene. *Error bars* represent the standard errors of duplicate microcosms. *Different letters above the bars* indicate a significant difference ($P<0.05$), *lowercase letters* for nitrite-N, *capital letters* for nitrate-N in **a**. Group "12C-x" and "13C-x" represent, respectively, the microcosms adding ^{12}C or ^{13}C as the inorganic carbon source with ammonia concentration of "x" mg L^{-1}

N but decreased evidently in microcosms with 20 mg L^{-1} NH_4^+-N. The abundance of bacterial *amoA* gene increased in all groups of microcosms during the cultivation (Fig. 5c). The increment of bacterial *amoA* gene in the 20 mg L^{-1} NH_4^+-N microcosm was significantly higher than that in the microcosm with 0.1 mg L^{-1} NH_4^+-N.

The relative proportions of both *amoA* genes in the fractions after density gradient centrifugation of DNA were illustrated in Fig. 6. Before the cultivation, the archaeal and bacterial *amoA* genes reached the maximum proportions in light fractions of buoyant densities around 1.68 and 1.69 mg L^{-1}, respectively. In the ^{12}C-$NaHCO_3$ treatment, the abundance peaks of archaeal and bacterial *amoA* genes did not shift throughout the whole incubation at both 0.1 and 20 mg L^{-1} NH_4^+-N concentrations. In the ^{13}C-$NaHCO_3$ treatment, a clear shift of archaeal *amoA* gene abundance was observed only at 0.1 mg L^{-1} NH_4^+-N concentration that the peak moved to heavy fractions with a final buoyant density around 1.71 mg L^{-1} at both day 28 and 56; while under the same low NH_4^+-N condition, the shift of bacterial *amoA* gene abundance was not evident at day 28 but became clear at day 56 that the peak moved to the heavy fraction of buoyant density around 1.72 mg L^{-1}, and under the high NH_4^+-N condition of 20 mg L^{-1}, only the peak of bacterial *amoA* gene abundance exhibited a clear-cut shift to heavy fractions with a buoyant density around 1.72 mg L^{-1} at both days 28 and 56.

Diversities of active AOA and AOB in different microcosms

After 56 days incubation under different ammonia concentrations, the archaeal and bacterial *amoA* genes in the cDNA samples as well as in the DNA samples of the heavy fractions in the ^{13}C-$NaHCO_3$-treated microcosms were analyzed by pyrosequencing.

For AOA, owning to the low abundance of archaeal *amoA* in the cDNA sample from group A12 and in the DNA-SIP sample of the heavy fraction from group ^{13}C-20, no target product was obtained by the PCR amplification. Thus, five pyrosequencing libraries of archaeal *amoA* gene from A0, A0.1, A2, A6, and ^{13}C-0.1 were constructed. The estimations and the rarefaction curves of the five libraries were shown in Table S5 and Fig. S1, respectively. A total of 126 OTUs were obtained from 8916 sequences. The main OTUs of archaeal

Fig. 6 Distribution of the relative abundance of archaeal and bacterial *amoA* genes in CsCl gradient for the DNA-SIP microcosms. Fourteen fractions of genomic DNA extracted from centrifuge tubes covered a range of buoyant density from 1.66 to 1.76 g mL^{-1}. The *vertical axis* reveals the proportion of AOA or AOB *amoA* gene in each fraction to the total abundance of a gradient set. *Vertical and horizontal error bars* represent, respectively, the standard errors of the relative abundance and buoyant density from triplicate detection of each fraction sample

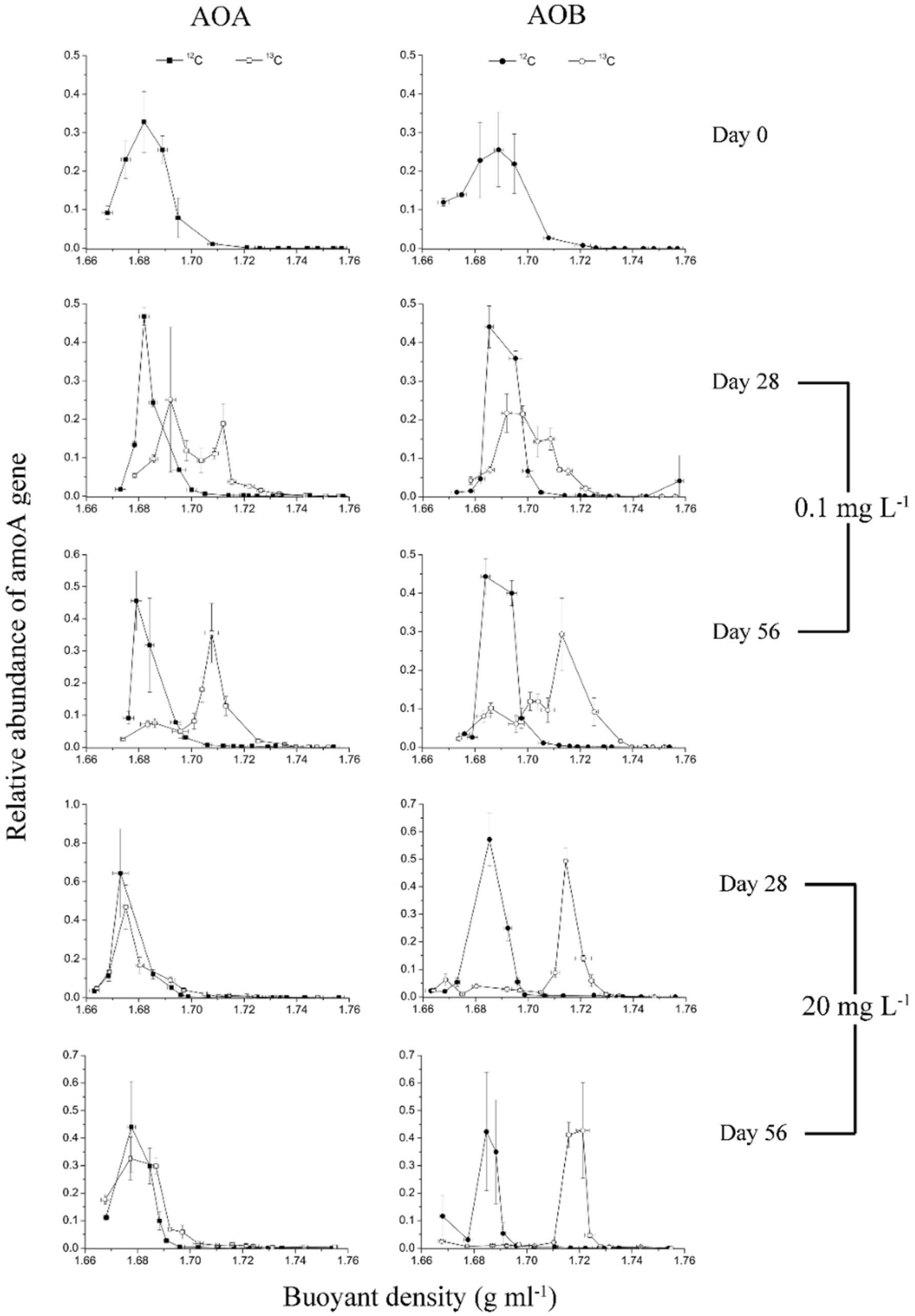
AOA
AOB
^{12}C
^{13}C
Day 0
Day 28
Day 56
0.1 mg L^{-1}
Day 28
Day 56
20 mg L^{-1}
Relative abundance of amoA gene
Buoyant density (g ml^{-1})

amoA gene (Fig. S2) from different microcosms were assorted by phylogenetic tree. As shown in Fig. S3, all detected AOA OTUs were placed into four clusters of *Nitrosopumilus maritimus*. The distribution and relative abundance of the detected AOA clusters were further analyzed (Fig. 7a). The main active AOA in A0 were *N. maritimus* C12 sister and *N. maritimus* SCM1 clusters, accounted for 48.1 and 44.0 % of the total sequences, respectively. With ammonia increased, *N. maritimus* C12 sister gradually increased to over 80 %; however *N. maritimus* SCM1 cluster decreased sharply and finally disappeared. Different composition of AOA was found in ^{13}C-0.1, where *N. maritimus* A10, *N. maritimus* C12, and *N. maritimus* C12 sister clusters accounted for 66.9, 24.9, and 1.9 %, respectively.

For AOB, owning to the low abundance of bacterial *amoA* gene in A0 and A0.1, no target product was obtained by the amplification. Thus, six pyrosequencing libraries of bacterial *amoA* gene from A2, A6, A12, A20, ^{13}C-0.1, and ^{13}C-20 were constructed by pyrosequencing. The estimations and the rarefaction curves of the six libraries were shown in Table S6 and Fig. S4, respectively. A total of 168 OTUs were obtained from 15,129 sequences. The main OTUs of bacterial *amoA* gene (Fig. S5) from different microcosms were also assorted by phylogenetic tree. As shown in Fig. S6, the detected AOB OTUs were placed into five clusters of genus *Nitrosomonas* and one cluster of genus *Nitrosospira*. The distribution and relative abundance of the detected AOB clusters were also analyzed (Fig. 7b). In A2, *Nitrosomonas oligotropha* and *Nitrosomonas nitrosa* clusters accounted for 61.2 and 34.5 % in the total sequences, respectively. However, both clusters decreased equally in A6 and A12 and almost disappeared in A20. *Nitrosomonas communis* cluster became the main active AOB under high ammonia conditions, which accounted for 42.2, 48.5, and 95.1 % in A6, A12, and A20,

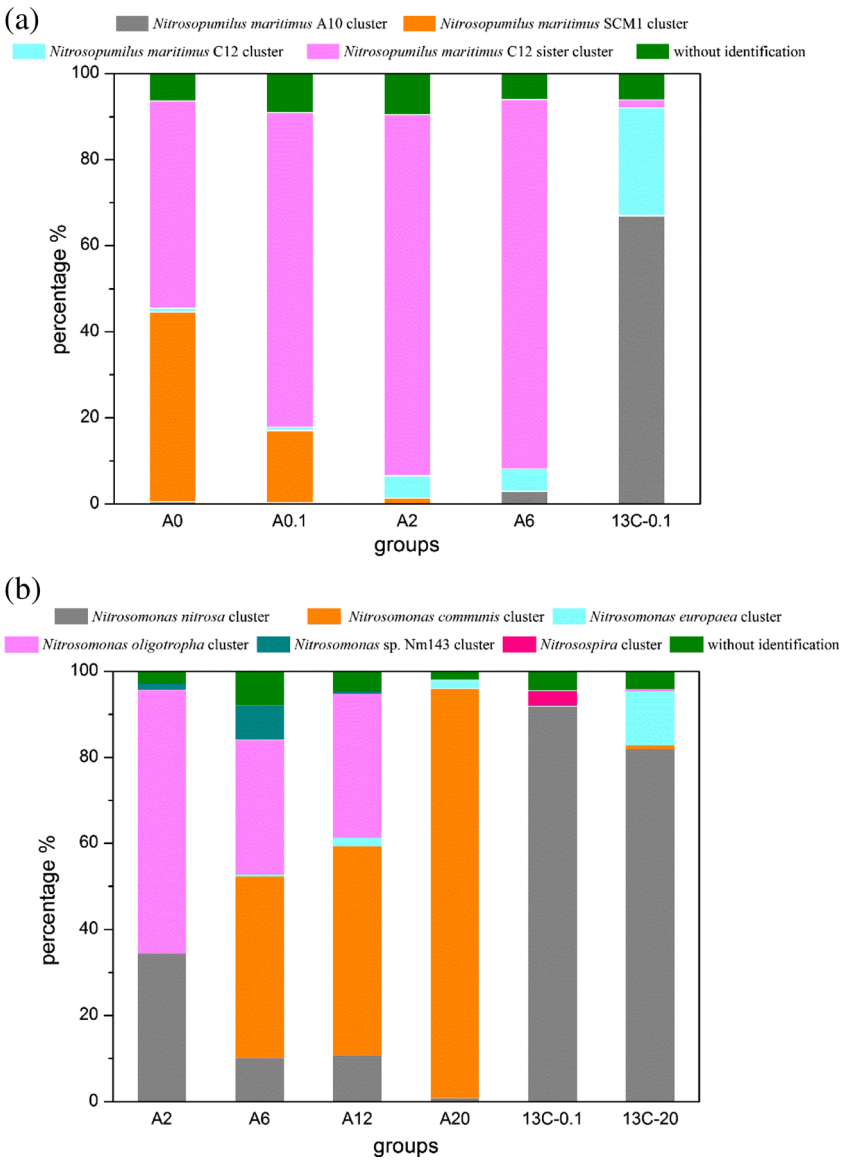

Fig. 7 Distribution and relative abundance of the phylogenetic AOA and AOB groups. The group without identification consists of the OTUs that accounted for less than 1 % of the total sequences in the pyrosequencing library. **a** Phylogenetic AOA groups and **b** phylogenetic AOB groups

respectively. In DNA-SIP microcosms, the composition of ^{13}C-labeled AOB *amoA* gene were markedly different, as *N. nitrosa* cluster was absolutely the dominant AOB in both ^{13}C-0.1 and ^{13}C-20.

Discussion

In this study, a series of coastal sediment-water microcosms with different ammonia concentrations were incubated. The nitrite and nitrate in the non-SIP microcosms (Fig. 1) and SIP microcosms (Fig. 5a) demonstrated the achievement of nitrification. The total amount of nitrite and nitrate increased with the improvement of ammonia concentration, indicating that the ammonia oxidation capacity of the sediment was enhanced in ammonia-rich environments. However, nitrite accumulation implied that nitrification was incomplete in the high ammonia groups, which might be due to the insufficient IC source according to the chemolithotrophy of nitrite oxidizer (Xia et al. 2011). The less accumulation of nitrite in the SIP microcosms (Fig. 5a), which were supplemented with external bicarbonate, supported this deduction.

A strong evidence for ammonia concentration effecting on the activities of AOA and AOB in aquatic environments was provided by this study. First, the positive correlations between the abundance of AOB *amoA* gene, not AOA *amoA* gene, and ammonia concentration were revealed in this study (Fig. 3). These indicated that ammonia may stimulate the growth of AOB in the NH_4^+-N concentration range studied. However, the linear regressions were obstructed by the lower abundance of AOB *amoA* gene in group A20 at day 56 (Fig. 2), which was probably a result of the inhabitation of AOB growth by highly accumulated nitrite (Fig. 1), as nitrite exerts inhibitory effect on the respiration rate of AOB (Contreras et al. 2008). The negative correlation between the archaeal *amoA* gene abundance in day 28 and the NH_4^+-N concentration indicated that in the NH_4^+-N concentration range studied, higher NH_4^+-N concentration may inhibit the growth of AOA. However, a moderate positive correlation was found between AOA abundance and the NH_4^+-N concentration in day 56. The recovered AOA was related with the accumulated nitrite in the microcosms (Fig. 1). We deduced that the growth of AOA might be promoted by the highly accumulated nitrite in the microcosm through "nitrifier denitrification" using copper-containing nitrite reductase (*nirK*), which has been proved widespread in AOA (Blainey et al. 2011; Lund et al. 2012; Walker et al. 2010).

Second, the ratio of the transcribed AOB/AOA *amoA* gene increased from 0.1 in low ammonia microcosms (group A0 and A0.1) to 43 in high ammonia microcosm (group A12), and the transciption of AOA *amoA* even was not detected in the highest ammonia microcosm (group A20) (Fig. 4).

Third, the incorporation of ^{13}C into genomic DNA revealed inconsistent growth and activity between AOA and AOB at both low and high ammonia concentration (Fig. 5). In the microcosms with 0.1 mg L^{-1} NH_4^+-N, both AOA and AOB involved in nitrification as the peaks of archaeal and bacterial *amoA* genes shifted to a heavy fractions of buoyant densities (Fig. 6). Nevertheless, the slower shift rate of the peak of AOB *amoA* gene was consistent with the less AOB *amoA* gene in cDNA (Fig. 4), indicating that AOA exerted higher ammonia oxidation activity than AOB at the lower ammonia concentration. In the microcosms with 20 mg L^{-1} NH_4^+-N, the stability of the peak of AOA *amoA* gene (Fig. 6) indicated the inhibited nitrifying activity of AOA, which was in good agreement with the undetected AOA *amoA* gene in cDNA (Fig. 4). Consistently, the abundance of AOA *amoA* gene in SIP microcosms was found decreased at the higher ammonia concentration (Fig. 5b). Therefore, AOA plays a more important role in ammonia oxidation in the ammonia-limited water environments (0.1 mg L^{-1}), while AOB thrives in the ammonia-rich ones (20 mg L^{-1}).

Pure culture experiments of AOA species also support the verdict, as AOA have low half-saturation constant and strong tolerance in minimal ammonia environments. The kinetic study of *N. maritimus* SCM1 obtained the lowest half-saturation constant (Km=133 nM) and the minimum ammonia concentration (less than 20 nM), which was over 100-fold lower than that required by AOB (Martens-Habbena et al. 2009). The growth of AOA strains were inhibited at certain thresholds of environmental ammonia concentration, e.g., *N. maritimus* SCM1, 2 mM (Martens-Habbena et al. 2009); *Nitrososphaera gargensis*, 3.08 mM (Hatzenpichler et al. 2008); *Nitrososphaera viennensis* EN76, 20 mM (Tourna et al. 2011), *Nitrosotalea devanaterra* Nd1, 20 mM (Lehtovirta-Morley et al. 2011), and AOA strain MY1, 50 mM (Jung et al. 2011). Those ammonia thresholds were significantly lower than the maximum ammonia tolerance (50–1000 mM) of the majority of AOB.

Although AOA may play a more important role in ammonia-limited aquatic environments, another discovery in this study is that the abundance of AOA and the transcribed AOA *amoA* gene increased as ammonia concentration was increased from 0.1 to 2 mg L^{-1} (Fig. 2a and Fig. 4). We consider that the ammonia oxidation activity of AOA would be inhibited only when the environmental ammonia exceeded a certain concentration, for example, 6 mg L^{-1} in this study.

Regarding the AOM species in the coastal microcosms, all detected AOA were *N. maritimus*. In contrast with the AOA strains isolated from soils (Lehtovirta-Morley et al. 2011; Tourna et al. 2011) and hot springs (de la Torre et al. 2008; Hatzenpichler et al. 2008), our study shows that AOA in different niches mainly belong to different lineages.

The composition of AOB was a little more complicated than that of AOA. The dominant active AOB gradually shifted

from *N. oligotropha* and *N. nitrosa* in A2 to *N. communis* in A20 (Fig. 7b). According to previous researches, the growth of *N. oligotropha* could be inhibited by low ammonia concentration similar to the AOA strain Candidatus *Nitrososphaera* sp. EN76 (Tourna et al. 2011); the half-saturation constant of *Nitrosomonas europaea* was 10 times higher than that of *N. oligotropha* (Martens-Habbena et al. 2009), and the activity of hydroxylamine-cytochrome *c* reductase (HCR, transforming hydroxylamine to nitrite) of *N. communis* strain YNSRA was twice higher than that of *N. europaea* ATCC25978T (Tokuyama et al. 2004). These explained the shift of the active AOB in our study.

Comparing the SIP microcosms with the non-SIP microcosms (Fig. 7), the potential active ammonia oxidizers detected in the heavy fractions were quite different from the active ammonia oxidizers measured in the RNA from non-SIP microcosms. This phenomenon may attribute to the influence of the supplement of inorganic carbon. In a recent study (Fukushima et al. 2013), *N. nitrosa* lineage was identified as the dominant AOB in the high-IC bioreactor (100 mg L^{-1} IC), while *N. europaea* increased in the low-IC bioreactor (15 mg L^{-1}). Likewise in the SIP microcosms in this study, the initial IC concentration was 100 mg L^{-1}, the dominant AOB cluster detected in heavy fractions was *N. nitrosa* lineage. In addition, nitrifier denitrification and other metabolic abilities of AOM undiscovered may be the reasons.

Taken together, our study provides solid evidence for the higher activity of AOA in lower ammonia concentration (NH_4^+-N≤0.1 mg L^{-1}) and AOB in higher ammonia concentration (NH_4^+-N≥2 mg L^{-1}) and showed the shift of diverse lineages of the active AOM with NH_4^+-N increasing from less than 0.1 to 20 mg L^{-1}. The results confirmed the effect of ammonia concentration on the AOM ecosystem and revealed the structures of AOM under different ammonia concentrations. The observation of inconformity between the transcribed and ^{13}C-labeled *amoA* genes suggests the complex metabolic pathways of the ammonia oxidizers, for which further research is need.

Acknowledgments This study was supported by a General Project (No. 51178002) granted by the Natural Science Foundation of China. The authors appreciate the great help from Zhejiang Provincial Zhoushan Marine Ecological Environmental Monitoring Station and Zhoushan Environmental Protection Bureau for the sampling sites' determination. The authors also thank Zhongyuan Zheng, Jing Zhang, Zhichao Li, Chengfeng Zhang from Peking University, Cong Liu from Tsinghua University, and Yin Zhang from Shanghai Normal University for helping in the sample collection.

Conflict of interest We declare that we have no conflicts of interest.

References

Adair KL, Schwartz E (2008) Evidence that ammonia-oxidizing archaea are more abundant than ammonia-oxidizing bacteria in semiarid soils of northern Arizona, USA. Microbiol Ecol 56(3):420–426

Arrigo KR (2005) Marine microorganisms and global nutrient cycles. Nature 437(7057):349–355

Bai Y, Shi Q, Wen D, Li Z, Jefferson WA, Feng C, Tang X (2012a) Bacterial communities in the sediments of Dianchi Lake, a partitioned eutrophic waterbody in China. PLoS ONE 7(5):e37796

Bai Y, Sun Q, Wen D, Tang X (2012b) Abundance of ammonia-oxidizing bacteria and archaea in industrial and domestic wastewater treatment systems. FEMS Microbiol Ecol 80(2):323–330

Beman JM, Popp BN, Francis CA (2008) Molecular and biogeochemical evidence for ammonia oxidation by marine Crenarchaeota in the Gulf of California. ISME J 2(4):429–441

Beman JM, Sachdeva R, Fuhrman JA (2010) Population ecology of nitrifying archaea and bacteria in the Southern California Bight. Environ Microbiol 12(5):1282–1292

Blainey PC, Mosier AC, Potanina A, Francis CA, Quake SR (2011) Genome of a low-salinity ammonia-oxidizing archaeon determined by single-cell and metagenomic analysis. PLoS ONE 6(2):e16626

Bouskill NJ, Eveillard D, Chien D, Jayakumar A, Ward BB (2012) Environmental factors determining ammonia-oxidizing organism distribution and diversity in marine environments. Environ Microbiol 14(3):714–729

Caffrey JM, Bano N, Kalanetra K, Hollibaugh JT (2007) Ammonia oxidation and ammonia-oxidizing bacteria and archaea from estuaries with differing histories of hypoxia. ISME J 1(7):660–662

Caporaso JG, Kuczynski J, Stombaugh J, Bittinger K, Bushman FD, Costello EK, Fierer N, Pena AG, Goodrich JK, Gordon JI, Huttley GA, Kelley ST, Knights D, Koenig JE, Ley RE, Lozupone CA, McDonald D, Muegge BD, Pirrung M, Reeder J, Sevinsky JR, Tumbaugh PJ, Walters WA, Widmann J, Yatsunenko T, Zaneveld J, Knight R (2010) QIIME allows analysis of high-throughput community sequencing data. Nat Methods 7(5):335–336

Contreras EM, Ruiz F, Bertola NC (2008) Kinetic modeling of inhibition of ammonia oxidation by nitrite under low dissolved oxygen conditions. J Environ Eng ASCE 134(3):184–190

de la Torre JR, Walker CB, Ingalls AE, Koenneke M, Stahl DA (2008) Cultivation of a thermophilic ammonia oxidizing archaeon synthesizing crenarchaeol. Environ Microbiol 10(3):810–818

Di HJ, Cameron KC, Shen J-P, Winefield CS, O'Callaghan M, Bowatte S, He J-Z (2010) Ammonia-oxidizing bacteria and archaea grow under contrasting soil nitrogen conditions. FEMS Microbiol Ecol 72(3):386–394

Di HJ, Cameron KC, Shen JP, Winefield CS, O'Callaghan M, Bowatte S, He JZ (2009) Nitrification driven by bacteria and not archaea in nitrogen-rich grassland soils. Nat Geosci 2(9):621–624

Francis CA, Roberts KJ, Beman JM, Santoro AE, Oakley BB (2005) Ubiquity and diversity of ammonia-oxidizing archaea in water columns and sediments of the ocean. Proc Natl Acad Sci U S A 102(41):14683–14688

Fukushima T, Whang L-M, Chiang T-Y, Lin Y-H, Chevalier LR, Chen M-C, Wu Y-J (2013) Nitrifying bacterial community structures and their nitrification performance under sufficient and limited inorganic carbon conditions. Appl Microbiol Biotechnol 97(14):6513–6523

Gao J-F, Luo X, Wu G-X, Li T, Peng Y-Z (2013) Quantitative analyses of the composition and abundance of ammonia-oxidizing archaea and ammonia-oxidizing bacteria in eight full-scale biological wastewater treatment plants. Bioresour Technol 138:285–296

Glaser K, Hackl E, Inselsbacher E, Strauss J, Wanek W, Zechmeister-Boltenstern S, Sessitsch A (2010) Dynamics of ammonia-oxidizing communities in barley-planted bulk soil and rhizosphere following

nitrate and ammonium fertilizer amendment. FEMS Microbiol Ecol 74(3):575–591

Hatzenpichler R, Lebedeva EV, Spieck E, Stoecker K, Richter A, Daims H, Wagner M (2008) A moderately thermophilic ammonia-oxidizing crenarchaeote from a hot spring. Proc Natl Acad Sci U S A 105(6):2134–2139

Jia Z, Conrad R (2009) Bacteria rather than archaea dominate microbial ammonia oxidation in an agricultural soil. Environ Microbiol 11(7): 1658–1671

Jung M-Y, Park S-J, Min D, Kim J-S, Rijpstra WIC, Damste JSS, Kim G-J, Madsen EL, Rhee S-K (2011) Enrichment and characterization of an autotrophic ammonia-oxidizing archaeon of mesophilic crenarchaeal group I.1a from an agricultural soil. Appl Environ Microbiol 77(24):8635–8647

Konneke M, Bernhard AE, de la Torre JR, Walker CB, Waterbury JB, Stahl DA (2005) Isolation of an autotrophic ammonia-oxidizing marine archaeon. Nature 437(7058):543–546

Kumar S, Nei M, Dudley J, Tamura K (2008) MEGA: a biologist-centric software for evolutionary analysis of DNA and protein sequences. Brief Bioinform 9(4):299–306

Le Roux X, Poly F, Currey P, Commeaux C, Hai B, Nicol GW, Prosser JI, Schloter M, Attard E, Klumpp K (2008) Effects of aboveground grazing on coupling among nitrifier activity, abundance and community structure. ISME J 2(2):221–232

Lehtovirta-Morley LE, Stoecker K, Vilcinskas A, Prosser JI, Nicol GW (2011) Cultivation of an obligate acidophilic ammonia oxidizer from a nitrifying acid soil. Proc Natl Acad Sci U S A 108(38):15892–15897

Leininger S, Urich T, Schloter M, Schwark L, Qi J, Nicol GW, Prosser JI, Schuster SC, Schleper C (2006) Archaea predominate among ammonia-oxidizing prokaryotes in soils. Nature 442(7104):806–809

Liu S, Shen L, Lou L, Tian G, Zheng P, Hu B (2013) Spatial distribution and factors shaping the niche segregation of ammonia-oxidizing microorganisms in the Qiantang River, China. Appl Environ Microbiol 79(13):4065–4071

Lund MB, Smith JM, Francis CA (2012) Diversity, abundance and expression of nitrite reductase (nirK)-like genes in marine thaumarchaea. ISME J 6(10):1966–1977

Martens-Habbena W, Berube PM, Urakawa H, de la Torre JR, Stahl DA (2009) Ammonia oxidation kinetics determine niche separation of nitrifying archaea and bacteria. Nature 461(7266):976–981

Molina V, Belmar L, Ulloa O (2010) High diversity of ammonia-oxidizing archaea in permanent and seasonal oxygen-deficient waters of the eastern South Pacific. Environ Microbiol 12(9):2450–2465

Mosier AC, Francis CA (2008) Relative abundance and diversity of ammonia-oxidizing archaea and bacteria in the San Francisco Bay estuary. Environ Microbiol 10(11):3002–3016

Neufeld JD, Vohra J, Dumont MG, Lueders T, Manefield M, Friedrich MW, Murrell JC (2007) DNA stable-isotope probing. Nat Protoc 2(4):860–866

Pratscher J, Dumont MG, Conrad R (2011) Ammonia oxidation coupled to CO(2) fixation by archaea and bacteria in an agricultural soil. Proc Natl Acad Sci U S A 108(10):4170–4175

Schloss PD, Westcott SL, Ryabin T, Hall JR, Hartmann M, Hollister EB, Lesniewski RA, Oakley BB, Parks DH, Robinson CJ, Sahl JW, Stres B, Thallinger GG, Van Horn DJ, Weber CF (2009) Introducing mothur: open-source, platform-independent, community-supported software for describing and comparing microbial communities. Appl Environ Microbiol 75(23):7537–7541

Tokuyama T, Mine A, Kamiyama K, Yabe R, Satoh K, Matsumoto H, Takahashi R, Itonaga K (2004) *Nitrosomonas communis* strain YNSRA, an ammonia-oxidizing bacterium, isolated from the reed rhizoplane in an aquaponics plant. J Biosci Bioeng 98(4):309–312

Tourna M, Stieglmeier M, Spang A, Koenneke M, Schintlmeister A, Urich T, Engel M, Schloter M, Wagner M, Richter A, Schleper C (2011) *Nitrososphaera viennensis*, an ammonia oxidizing archaeon from soil. Proc Natl Acad Sci U S A 108(20):8420–8425

Venter JC, Remington K, Heidelberg JF, Halpern AL, Rusch D, Eisen JA, Wu DY, Paulsen I, Nelson KE, Nelson W, Fouts DE, Levy S, Knap AH, Lomas MW, Nealson K, White O, Peterson J, Hoffman J, Parsons R, Baden-Tillson H, Pfannkoch C, Rogers YH, Smith HO (2004) Environmental genome shotgun sequencing of the Sargasso Sea. Science 304(5667):66–74

Verhamme DT, Prosser JI, Nicol GW (2011) Ammonia concentration determines differential growth of ammonia-oxidising archaea and bacteria in soil microcosms. ISME J 5(6):1067–1071

Walker CB, de la Torre JR, Klotz MG, Urakawa H, Pinel N, Arp DJ, Brochier-Armanet C, Chain PSG, Chan PP, Gollabgir A, Hemp J, Huegler M, Karr EA, Koenneke M, Shin M, Lawton TJ, Lowe T, Martens-Habbena W, Sayavedra-Soto LA, Lang D, Sievert SM, Rosenzweig AC, Manning G, Stahl DA (2010) *Nitrosopumilus maritimus* genome reveals unique mechanisms for nitrification and autotrophy in globally distributed marine crenarchaea. Proc Natl Acad Sci U S A 107(19):8818–8823

Wang X, Wen X, Xia Y, Hu M, Zhao F, Ding K (2012) Ammonia oxidizing bacteria community dynamics in a pilot-scale wastewater treatment plant. PLoS ONE 7(4):e36272

Wessen E, Soderstrom M, Stenberg M, Bru D, Hellman M, Welsh A, Thomsen F, Klemedtson L, Philippot L, Hallin S (2011) Spatial distribution of ammonia-oxidizing bacteria and archaea across a 44-hectare farm related to ecosystem functioning. ISME J 5(7): 1213–1225

Wu Y, Xiang Y, Wang J, Zhong J, He J, Wu QL (2010) Heterogeneity of archaeal and bacterial ammonia-oxidizing communities in Lake Taihu, China. Environ Microbiol Rep 2(4):569–576

Wuchter C, Abbas B, Coolen MJL, Herfort L, van Bleijswijk J, Timmers P, Strous M, Teira E, Herndl GJ, Middelburg JJ, Schouten S, Damste JSS (2006) Archaeal nitrification in the ocean. Proc Natl Acad Sci U S A 103(33):12317–12322

Xia W, Zhang C, Zeng X, Feng Y, Weng J, Lin X, Zhu J, Xiong Z, Xu J, Cai Z, Jia Z (2011) Autotrophic growth of nitrifying community in an agricultural soil. ISME J 5(7):1226–1236

Zhang L-M, Offre PR, He J-Z, Verhamme DT, Nicol GW, Prosser JI (2010) Autotrophic ammonia oxidation by soil thaumarchaea. Proc Natl Acad Sci U S A 107(40):17240–17245